24. Ruoff, A. L. & Ghandehari, K. The refractive index of hydrogen as a function of pressure. *Mod. Phys. Lett. B* **7,** 907–911 (1993).
25. Hemley, J. R., Hanfland, M. & Mao, H. K. High pressure dielectric measurements of solid hydrogen to 170 GPa. *Nature* **350,** 488–491 (1991).
26. Straus, D. M. & Ashcroft, N. W. Self-consistent structure of metallic hydrogen. *Phys. Rev. Lett.* **38,** 415–418 (1997).
27. Richardson, C. F. & Ashcroft, N. W. High temperature superconductivity in metallic hydrogen; electron-electron enhancements. *Phys. Rev. Lett.* **78,** 118–121 (1997).
28. Kresse, G. & Hafner, J. Efficient iterative schemes for ab initio total energy calculations using a plane-wave basis set. *Phys. Rev. B* **54,** 11169–11186 (1996).
29. Vanderbilt, D. Soft self-consistent pseudopotentials in a generalized eigenvalue formalism. *Phys. Rev. B* **41,** 7892–7895 (1990).
30. Johnson, K. *Electronic Structure, Band-gaps, and the Insulator-metal Transition in Solid Hydrogen.* Thesis, Cornell Univ. (1998).

Acknowledgements

The results we report here were obtained using both the Vienna Ab-Initio Simulation Package authored by G. Kresse, J. Furthmüller and J. Hafner and the Corning Planewave code made available by M. Teter. We thank the Cornell Center for Materials Research for computing facilities. This work was supported by the US NSF.

Correspondence and requests for materials should be addressed to N.W.A. (e-mail: nwa@ccmr.cornell.edu).

Direct measurement of electrical transport through DNA molecules

Danny Porath*, Alexey Bezryadin*†, Simon de Vries* & Cees Dekker*

** Department of Applied Sciences, Delft University of Technology, 2628 CJ Delft, The Netherlands*

Attempts to infer DNA electron transfer from fluorescence quenching measurements[1–9] on DNA strands doped with donor and acceptor molecules have spurred intense debate[10,11] over the question of whether or not this important biomolecule is able to conduct electrical charges. More recently, first electrical transport measurements on micrometre-long DNA 'ropes'[12], and also on large numbers of DNA molecules in films[13], have indicated that DNA behaves as a good linear conductor. Here we present measurements of electrical transport through individual 10.4-nm-long, double-stranded poly(G)-poly(C) DNA molecules connected to two metal nanoelectrodes, that indicate, by contrast, large-bandgap semiconducting behaviour. We obtain nonlinear current–voltage curves that exhibit a voltage gap at low applied bias. This is observed in air as well as in vacuum down to cryogenic temperatures. The voltage dependence of the differential conductance exhibits a peak structure, which is suggestive of the charge carrier transport being mediated by the molecular energy bands of DNA.

The common model for electron transfer through DNA is based on overlap between π orbitals in adjacent base pairs[14]. Irregular base-pair sequences may lead to localization of charge carriers and reduce the transfer rate of electrons[9,15]. A structure containing a single type of base pair may therefore furnish the best conditions for π overlap. In our experiments, we used 10.4-nm-long (30 base pairs) poly(G)-poly(C) DNA oligomers, well characterized by ultraviolet measurements, mass spectrometry and gel electrophoresis. The 10.4-nm size is adequate to span two closely spaced metal nanoelectrodes as a linear, nearly stiff structure. A DNA molecule was positioned between the nanoelectrodes by electrostatic trapping (see Fig. 1 legend for details) from a dilute aqueous buffer containing about one molecule per $(100\,\mathrm{nm})^3$. This technique was developed for the trapping of single molecules, and has been shown to be successful for a variety of nanoparticles[16,17]. After a DNA molecule was trapped from the solution, the device was dried in a flow of nitrogen and electrical transport was measured. No current was measured between the bare electrodes before trapping the DNA, indicating that no short-circuit, breakdown or field emission occurs in the voltage range investigated (as checked up to 5 V for every sample and occasionally up to 10 V).

Here we report current–voltage (I–V) measurements on DNA oligomers. The current is essentially zero (<1 pA) up to a threshold voltage of a few volts. This shows that this system behaves as an insulator at low bias. Beyond the threshold the current rises sharply, showing that DNA can transport charge carriers. Relatively large currents can be supported by the DNA molecule: we occasionally put more than 100 nA through our device, which corresponds to a high rate, $\sim 10^{12}$ electrons s^{-1}, over the 10-nm-long molecule. Note, however, that our experiments involve electron transport rather than electron transfer (the latter describes a one-step tunnelling process). Subsequent current–voltage measurements under the same conditions yield similar characteristics, but with a variation of the width of the voltage gap (Fig. 1). Similar results were obtained for more than 20 different samples at ambient conditions.

A number of control experiments were performed. To verify that we indeed trap DNA and no other (in)organic particles, we

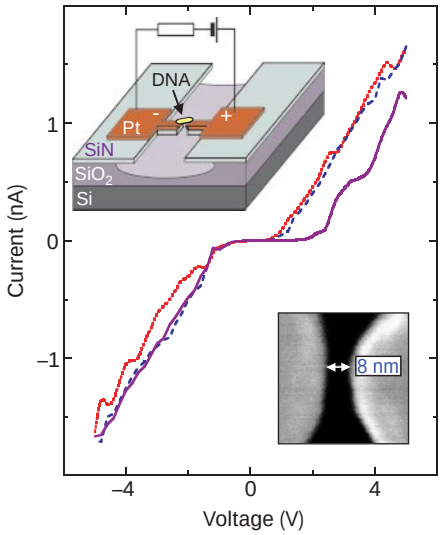

Figure 1 Current–voltage curves measured at room temperature on a DNA molecule trapped between two metal nanoelectrodes. The DNA molecule (30 base pairs, double-stranded poly(G)-poly(C)) is 10.4 nm long, and the nanoelectrodes are separated by 8 nm. Subsequent I–V curves (different colours) show similar behaviour but with a variation of the width of the voltage gap. Note that the conductance in these measurements is limited by a 2 GΩ series resistor. Air humidity is 50%. The upper inset shows a schematic of our sample layout. Using electron-beam lithography, we create a local 30-nm narrow segment in a slit in the SiN layer. Underetching the SiO_2 layer leads to two opposite free-standing SiN 'fingers' that become the metallic nanoelectrodes after sputtering Pt through a Si mask. The lower inset is a scanning-electron-microscope image of the two metal electrodes (light area) and the 8-nm gap between them (dark area). Details of fabrication and trapping are given elsewhere[16,17]. DNA was prepared in a buffer composition of 300 mM NaCl, 10 mM Na citrate and 5 mM EDTA (Eurogentec Bel S.A.). Deposition of a DNA molecule between the electrodes was achieved with electrostatic trapping[16,17]. A 1-μl droplet of dilute DNA solution is positioned on top of the sample, and a voltage of up to 5 V is then applied between the electrodes. The electrostatic field polarizes a nearby molecule, which is then attracted to the gap between the electrodes owing to the field gradient. When a DNA molecule is trapped and current starts to flow through it, a large part of the voltage drops across the series resistor, which reduces the field between the electrodes and prevents other molecules from being trapped[16,17]. Trapping of DNA molecules using this method is almost always successful.

† Present address: Physics Department, Harvard University, Cambridge, Massachusetts 02138, USA.

incubated a sample with trapped DNA (Fig. 2, solid curve) in a solution containing DNAse I, an enzyme that specifically cuts double-stranded DNA. After the DNAse I treatment, no significant current was observed (Fig. 2, dashed curve), indicating that the electrodes were indeed originally connected by DNA. In a complementary experiment, we repeated the same procedure using a similar enzyme solution but without the Mg ions that are needed to activate the enzyme. In this experiment the general shape of the curve did not change (Fig. 2, inset), confirming that in the original control experiment the DNA was indeed cut by the DNase I enzyme.

The length selectivity of the trapping procedure was checked by attempting to trap 10.4-nm-long chains between electrodes separated by 12 nm instead of 8 nm. Lack of success indicates that the DNA is trapped with its long axis bridging the two electrodes, and that it is very unlikely that we have measured conductance through two or more molecules in series, or through a number of parallel DNA chains 'sandwiched' between the electrodes, where each chain has its axis perpendicular to the line connecting the electrodes. Scanning-electron-microscope imaging of the gap between the electrodes after trapping a DNA molecule showed a very small amount of material (compared to the gap size) between the electrodes, probably amorphous carbon covering the DNA during the imaging process. Imaging of the bare electrodes before trapping the DNA did not show this material. The very low concentration of molecules in the solution, the trapping procedure (using a 2 GΩ series resistor), and the imaging together suggest that only a single DNA molecule, or at most a few, becomes trapped.

We also tried to trap from a droplet of buffer solution without DNA. Nothing was trapped in this case, and no conduction by ions or molecules present in the buffer solution was observed. I–V measurements performed in vacuum ($\sim 10^{-6}$ mbar) and below −20 °C exclude the possibility of ionic conduction through traces of water around the molecule[18], and confirm that the current is flowing through the DNA.

Three samples were measured in vacuum and at low temperatures down to 4 K. The differential conductance dI/dV versus V (Fig. 3a) exhibits a peak structure, with a peak spacing of 0.1–0.5 eV and a peak width of ~0.2 eV (typical values from many such curves). This structure is stable and reproducible over time, as can be seen from the close similarity of the six subsequent curves plotted in Fig. 3a. But after a number of I–V measurements (inset, blue line) we observe an abrupt change in the shape of the I–V curves: the new, stable and reproducible shape is shown as a pink line in the inset. Changes between stable configurations can be induced by an abrupt switch of the applied voltage or by a high current. Measurements at higher bias voltages (beyond the scale of Fig. 3a) also manifest a peak structure, but with more fluctuations and less reproducibility. The voltage gap in the I–V curves widens on increasing the temperature, as shown in Fig. 4. We do not yet understand this intriguing trend, which was observed for three different samples in both cooling and heating runs. The thermal expansion of the gap between the electrodes is very small (of the order of 1 Å), but may conceivably have some effect.

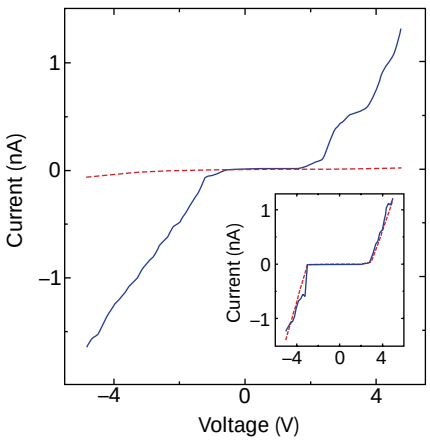

Figure 2 Current–voltage curves that show that transport is indeed measured on DNA trapped between the electrodes. The solid curve is measured after trapping a DNA molecule as in Fig. 1. The dashed curve is measured after incubation of the same sample for 1 h in a solution with 10 mg ml^{-1} DNAse I enzyme (5 mM Tris-HCl, 5 mM $MgCl_2$, 10 mg ml^{-1} DNAse I (pH 7.5)). The suppression of the current indicates that the double-stranded DNA was cut by the enzyme. This experiment was performed for four different samples (including the sample of Fig. 3a). Inset, two curves measured in a complementary experiment where the above procedure was repeated but in the absence of the Mg^{2+} ions that activate the enzyme and in the presence of 10 mM EDTA (ethylenediamine tetraacetic acid) that complexes any residual Mg ions. In this case, the shape of the curve did not change. This verifies that the DNA was indeed cut by the enzyme in the original control experiment.

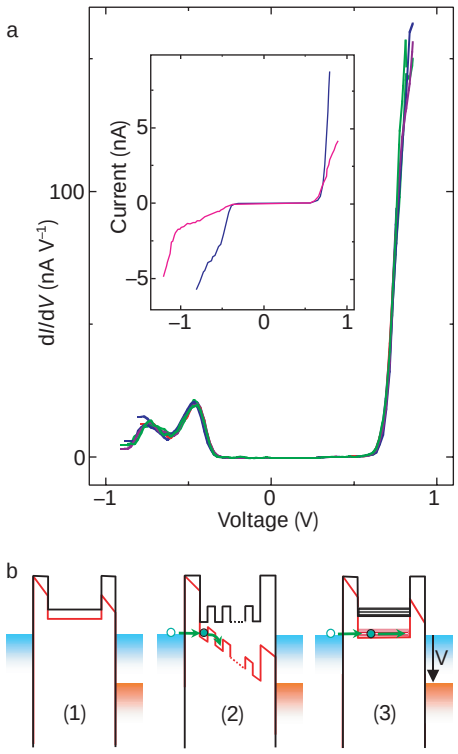

Figure 3 Differential conductance dI/dV versus applied voltage V at 100 K (**a**), and various models for the transport (**b**). **a**, The differential conductance shows a clear peak structure. Good reproducibility can be seen from the six nearly overlapping curves. The peak structure suggests that electron transport is mediated by the DNA molecular energy bands. Peak structures were observed in all three samples measured at low temperatures, although details were different from sample to sample. The dI/dV data were obtained by numerical derivation of the I–V curves. Subsequent sets of I–V measurements can show a sudden change, possibly due to conformational changes of the DNA. Inset, an example of two typical I–V curves that were measured before and after such an abrupt change. Switching between stable and reproducible shapes can occur after an abrupt switch of the voltage or by high current. The I–V curves were measured without a series resistor. **b**, Three basic models for transport through DNA. The black and red lines illustrate the situation with an without an applied bias voltage V, respectively. The contact between the DNA and the metal electrodes is represented by tunnelling barriers. The middle part describes the electronic states of the DNA. Model 1 describes unistep tunnelling, as commonly discussed in electron-transfer studies, model 2 describes sequential hopping between localized states, and model 3 describes molecular band conduction.

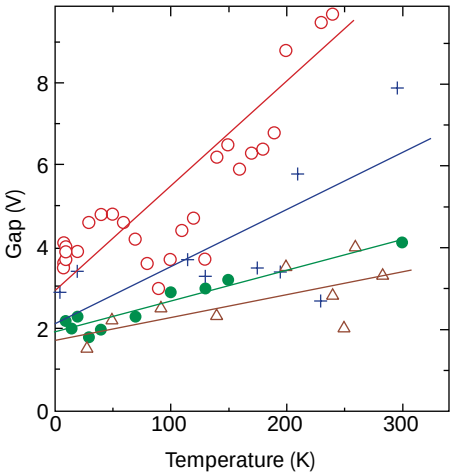

Figure 4 Temperature dependence of the voltage gap in the *I*–*V* curves for three different samples. The top two data sets (open circles and crosses) show results from two samples; the lower two data sets are cooling and heating measurements on a third sample. Solid lines are linear fits. The voltage gap is defined by the voltage at which the current rises above 1 pA. The voltage gap appears to widen with increasing temperature.

We now consider how these data relate to available models for electron transport through DNA. Figure 3b schematically outlines three models. The first is a one-step electron transfer process that involves tunnelling from electrode to electrode[8,9]. This can be ruled out in our samples owing to the very large tunnelling distance that would be involved (8 nm) and the large currents observed. The second model describes sequential hopping between localized states[7,8], which could, for example, be associated with the base pairs. The hopping process could be either unidirectional or involve one-dimensional diffusion. It can be argued that the back-and-forth diffusive hopping[8] is less likely in our case due to the high electric fields used, which will tilt the potential, and the high electron-transfer rates observed. (A calculation of the time needed for such diffusive motion along the chain limits the electron transfer rate to a value well below the one we observe.) In the third model, electronic interactions between the bases in the DNA molecule lead to a molecular band where the electronic states are delocalized over the entire length of the molecule. Electron transport in the hopping and band models is facilitated when the Fermi level of the electrode is aligned with the band edge by applying the bias voltage. Once electrons are injected, transport occurs through hopping or band conduction. (Holes rather than electrons may be the relevant carriers, but the physical picture of the transport process is essentially the same.)

The nature of the contact resistance between the DNA and the metal electrodes is not known. However, it is very likely that there is no good metallic contact[19] and that the contacts can be represented by tunnelling barriers. If the applied voltage drops largely across these barriers, the differential conductance dI/dV is determined by a combination of the electronic density of states of the DNA molecule and Coulomb blockade effects[20]. These effects are observed when the capacitance C of an object is so small that the addition of a single electron costs a charging energy $e^2/2C$ that is larger than the thermal energy. Coulomb blockade may lead to a voltage gap and steps in the I–V curve. For a 10-nm-long DNA molecule with states delocalized over the whole molecule, we estimate $C \sim 1$ aF and $e^2/2C \approx 0.2$ V, which is one order of magnitude smaller then the voltage gap observed in our measurements. Neither do we observe clear periodic Coulomb steps in the I–V curves. Although Coulomb blockade is thus likely to make a minor contribution to the gap in this case, it cannot solely explain it.

In the simplest hopping model, the DNA may alternatively be considered as a series of 30 very tiny (<3 Å) quantum dots. Each of these dots has a large charging energy (>5 V), and their series addition would lead to an even larger overall charging energy. This would lead to a Coulomb blockade voltage gap that is again incompatible with the data. Larger quantum dots formed from assemblies of adjacent base pairs may be considered, but this is not likely for our homogeneous poly(G)-poly(C) DNA where an extended model is more reasonable. We thus conclude that most of the observed gap probably originates from the offset between the Fermi level of the electrode and the molecular energy bands of the DNA molecule. The peaks in our curves then reflect the structure of the molecular bands of the DNA[21,22]. □

Received 25 June; accepted 3 December 1999.

1. Arkin, M. R. *et al.* Rates of DNA mediated electron transfer between metallointercalators. *Science* **273,** 475–480 (1996).
2. Lewis, F. D. *et al.* Distance-dependent electron transfer in DNA hairpins. *Science* **277**, 673–676 (1997).
3. Barbara, P. F. & Olson, E. J. C. Ch. 13 (Advances in Chemical Physics Vol. 107, Wiley & Sons, 1999).
4. Meggers, E., Michel-Beyerle, M. E. & Giese, B. Sequence dependent long range hole transport in DNA. *J. Am. Chem. Soc.* **120,** 12950–12955 (1998).
5. Beratan, D. N., Priyadarshy, S. & Risser, S. M. DNA: insulator or wire? *Chem. Biol.* **4,** 3–8 (1997).
6. Wan, C. *et al.* Femtosecond dynamics of DNA mediated electron transfer. *Proc. Natl Acad. Sci. USA* **96,** 6014–6019 (1999).
7. Henderson, P. T., Jones, D., Hampikian, G., Kan, Y. & Shuster, B. G. Long-distance charge transport in duplex DNA: the phonon-assisted polaron-like hopping mechanism. *Proc. Natl Acad. Sci. USA* **96,** 8353–8358 (1999).
8. Jortner, J., Bixon, M., Langenbacher, T. & Michel-Beyerle, M. E. Charge transfer and transport in DNA. *Proc. Natl Acad. Sci. USA* **95,** 12759–12765 (1998).
9. Grozema, F. C., Berlin, Y. A. & Siebbeles, L. D. A. Sequence dependent charge transfer in donor-DNA-acceptor systems: a theoretical study. *Int. J. Quant. Chem.* **75,** 1009–1016 (1999).
10. Taubes, G. Double helix does chemistry at a distance—but how? *Science* **275,** 1420–1421 (1997).
11. Wilson, E. K. DNA conductance still confounds. *Chem. Eng. News* 2751–2754 (1998).
12. Fink, H. W. & Schönenberger, C. Electrical conduction through DNA molecules. *Nature* **398,** 407–410 (1999).
13. Okahata, Y., Kobayashi, T., Tanaka, K. & Shimomura, M. Anisotropic electric conductivity in an aligned DNA cast film. *J. Am. Chem. Soc.* **120,** 6165–6166 (1998).
14. Elley, D. D. & Spivey, D. I. Semiconductivity of organic substances. *Trans. Faraday Soc.* **58,** 411–415 (1962).
15. Hutter, M. & Clark, T. On the enhanced stability of the guanine-cytosine base-pair radical cation. *J. Am. Chem. Soc.* **118,** 7574–7577 (1996).
16. Bezryadin, A. & Dekker, C. Nanofabrication of electrodes with sub-5 nm spacing for transport experiments on single molecules and metal clusters. *J. Vac. Sci. Technol. B* **15,** 793–799 (1997).
17. Bezryadin, A., Dekker, C. & Schmid, G. Electrostatic trapping of single conducting nanoparticles between nanoelectrodes. *Appl. Phys. Lett.* **71,** 1273–1275 (1997).
18. van Lith, D., Warman, J. M., de Haas, M. P. & Hummel, A. Electron migration in hydrated DNA and collagen at low temperatures. *J. Chem. Soc. Faraday Trans. 1* **82,** 2933–2943 (1986).
19. Datta, S. *et al.* Current-voltage characteristics of self-assembled monolayers by scanning tunneling microscopy. *Phys. Rev. Lett.* **79,** 2530–2533 (1997).
20. Grabert, H. & Devoret, M. H. *Single Charge Tunneling* (Plenum, New York, 1992).

21. Bakhshi, A. K. Investigation of electronic conduction in proteins and DNA. *Prog. Biophys. Mol. Biol.* **61,** 187–253 (1994).
22. Ladik, J. Energy bands in DNA. *Int. J. Quantum Chem.* **4,** 307–317 (1971).

Acknowledgements

We thank L. Gurevich for assistance in the fabrication and measurements; E. W. J. M. van der Drift, A. van der Enden, L. E. M. de Groot, S. G. Lemay, A. K. Langen-Suurling, R. N. Schouten, Z. Yao, T. Zijlstra, M. R. Zuiddam, M. P. de Haas, J. M. Warman, A. Storm, N. Kemeling and J. Jortner for assistance and discussions; and E. Kramer and E. Yildirim for the DNA characterization measurements. This work was supported by the Dutch Foundation for Fundamental Research on Matter (FOM).

Correspondence and requests for materials should be addressed to C.D. (e-mail: dekker@qt.tn.tudelft.nl.).

Non-destructive determination of local strain with 100-nanometre spatial resolution

S. Di Fonzo*, W. Jark*, S. Lagomarsino†, C. Giannini‡, L. De Caro‡, A. Cedola†§ & M. Müller§

** SINCROTRONE TRIESTE, SS 14 km 163.5 in Area Science Park, I-34012 Basovizza - Trieste, Italy*
† Istituto Elettronica Stato Solido (IESS) - CNR, V. Cineto Romano 42, I-00156 Roma, Italy
‡ Centro Nazionale Ricerca e Sviluppo Materiali (PASTIS-CNRSM), Strada Statale 7 Appia km 712, I-72100 Brindisi, Italy
§ ESRF, BP 220, F-38043 Grenoble Cedex, France

Structure sizes of ~180 nm are now standard in microelectronics, and state-of-the-art fabrication techniques can reduce these to just a few tens of nanometres (ref. 1). But at these length scales, the strain induced at interfaces can locally distort the crystal lattice, which may in turn affect device performance in an unpredictable way. A means of non-destructively characterizing such strain fields with high spatial resolution and sensitivity is therefore highly desirable. One approach is to use Raman spectroscopy[2], but this is limited by the intrinsic ~0.5-μm resolution limit of visible light probes. Techniques based on electron-beam diffraction can achieve the desired nanometre-scale resolution. But either they require complex sample preparation procedures[3] (which may alter the original strain field) or they are sensitive to distortional (but not dilational) strain within only the top few tens of nanometres of the sample surface[4,5]. X-rays, on the other hand, have a much greater penetration depth, but have not hitherto achieved strain analysis with sub-micrometre resolution[6]. Here we describe a magnifying diffraction imaging procedure for X-rays which achieves a spatial resolution of 100 nm in one dimension and a sensitivity of 10^{-4} for relative lattice variations. We demonstrate the suitability of this procedure for strain analysis by measuring the strain depth profiles beneath oxidized lines on silicon crystals.

The crucial element of our set-up is a waveguide[7,8] (WG in Fig. 1), which constitutes an unusual optical element for medium- and high-energy X-rays (10–30 keV). Unlike diffracting optical elements it does not focus a collimated incident beam, but instead confines it (through a resonance effect[9]) in one direction to a dimension of typically 100–150 nm, the distance between the parallel interfaces of the resonator[8]. Several resonator modes can be excited; these modes can leave at the end of the waveguide, with a high degree of spatial coherence in the plane perpendicular to the waveguide surface, which is here the vertical one. In this direction, the beam profile of the first resonance mode—at distances of more than 1 mm from the waveguide end—is well described by a gaussian beam[10,11]; this mode then seems to originate from a virtual line source inside the resonator. This has allowed us to register an in-line hologram with a spatial resolution of 140 nm in one direction[12].

The idea behind the present diffraction imaging experiment is as follows: for highly monochromatic X-rays, a perfect crystal has a limited angular acceptance (typically a few tens of microradians) in its diffraction plane, which in our geometry in Fig. 1 is the horizontal plane. But in the vertical plane, its angular acceptance is larger and can even exceed 1 mrad. This acceptance can be matched favourably with the characteristics of the waveguided beam, which is divergent (typically 1 mrad) in the vertical plane while maintaining its collimation in the horizontal plane. Strain sensitivity is then achieved with the collimated beam in the horizontal plane. High spatial resolution is utilized in the vertical direction, in which local structural variations at the sample are registered by projecting them, magnified, on a two-dimensional detector placed far from the sample. So spatial resolution and strain resolution are not correlated, as they are obtained in orthogonal directions: spatial resolution in the horizontal plane has to be sacrificed in order to obtain good strain sensitivity.

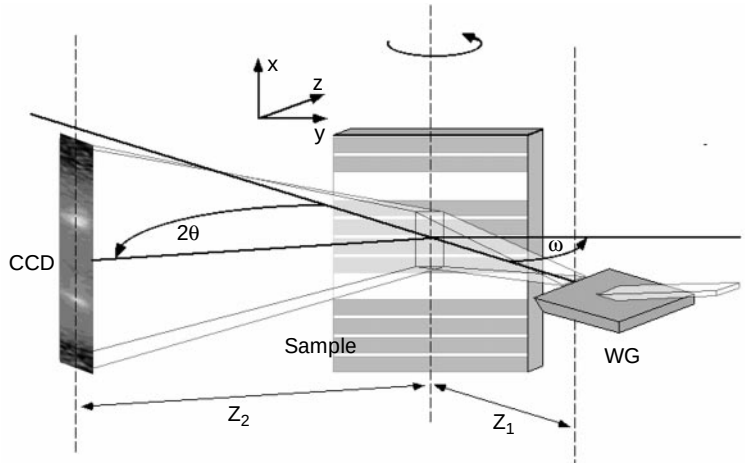

Figure 1 Diffraction imaging set-up. The beam arriving on the waveguide (WG) surface is spatially compressed by the waveguide in the vertical direction; the beam leaving the waveguide is vertically divergent. This latter beam, impinging on the sample surface at an incident angle ω, is diffracted in the horizontal plane towards the two-dimensional CCD detector positioned at a fixed scattering angle 2θ. The waveguide disperses the beam in the vertical plane providing at the CCD detector a magnification $M = (Z_1 + Z_2)/Z_1 \sim Z_2/Z_1$ for any structural variations occurring at the sample surface in this plane. Z_1 is the WG–sample distance, Z_2 is the sample–detector distance. In a Bragg scan only ω is varied.